Photodegradation of reactive red 141 by combined photocatalysis and photo-Fenton-like processes

Selma K.Kuriechen[1], Sepperumal Murugesan[2]*

[1]School of Energy, Environment & Natural Resources, Madurai Kamaraj University, Madurai-625 021, (INDIA)
[2]Dept. of Inorganic Chemistry, School of Chemistry, Madurai Kamaraj University, Madurai-625 021, (INDIA)
E-mail : smsan@mail.com

ABSTRACT

The present study investigates the photodegradation of a di-azo dye, Reactive Red 141 by combining photo-Fenton-like reactions (Fe^{3+} or Cu^{2+}) and TiO_2 or sulphur-doped TiO_2 (S-TiO_2) based heterogeneous photocatalysis. The mineralization efficiency of paired systems is evaluated from total organic carbon (TOC) measurements. The photodegradation rates of coupled systems are higher than those of individual techniques of photocatalysis and photo-Fenton-like reactions under visible light illumination. While the addition of metal-ions to the TiO_2-RR141 system reduces the rate of photodegradation of RR141, the metal-ions addition to TiO_2-oxone-RR141 system increases the degradation of RR141 due to synergistic effect.   © 2013 Trade Science Inc. - INDIA

KEYWORDS

Advanced oxidation processes;
Photocatalysis;
Photo-Fenton;
Photodegradation.

INTRODUCTION

Degradation of organic pollutants by pairing different oxidation processes has become a common practice. The competence of combined systems with photocatalysis and sonolysis or photocatalysis and membrane filtration or photo-Fenton reactions and sonolysis or electro- photo-Fenton[1–6] etc., are reported. But not many attempts were made in pairing photocatalysis and photo-Fenton-like reactions for wastewater treatment. The rate of photodegradation of pollutants in combined oxidation processes mainly depends on the reactive radical formation. In photocatalysis and photo-Fenton coupled systems, reactive radicals are generated by photocatalytic reactions on semiconductor photocatalysts as well as by the independent Fe(III)

aqua complexes through photo-redox reaction[7]. Application of photo-induced reactions using titanium dioxide (TiO_2) is limited due to its requirement for UV light for its excitation. Doping of TiO_2 with anion impurities[8–12] has been effective in lowering the threshold energy for photochemistry on the TiO_2 surface. Another factor that affects the efficiency of photocatalytic process is the recombination of photo-generated electrons and holes on the surface of the catalyst. However, it can be restrained by adding suitable scavengers of particular charge carriers. In photo-Fenton-like reactions, transition metals with two or more valence states with a suitable oxidation–reduction potential can be used to produce ·OH. Few reports are also found on the application of peroxomonosulphate (PMS or oxone)[13] and peroxodisulphate (PDS)[14] as oxidant instead of con-

Current Research Paper

ventional H_2O_2 along with metal ions in photo-Fenton-like reactions. These oxidants led to the generation of sulphate radicals (redox potential of 2.6 V) which had greater efficiencies in the presence of metal ion catalyst and light. In this study, photo-Fenton-like reactions (Fe^{3+} or Cu^{2+}-oxidants) are combined with TiO_2 or sulphur-doped TiO_2 (S-TiO_2) mediated photocatalysis and its efficiency under visible light in removing synthetic dye Reactive Red 141 (RR141) from wastewater streams are assessed.

EXPERIMENTAL

Materials

Widely used textile dye, Reactive Red 141 ($C_{52}H_{34}O_{26}S_8Cl_2N_{14}$; $\lambda_{max} = 543$ nm; $\varepsilon_{max} = 25,000$ M^{-1} cm^{-1}) is obtained from Supra Tulvers, India and was used as the model pollutant without further purification. Potassium peroxomonosulphate (PMS or oxone) was obtained from Sigma-Aldrich. Analytical grade ferric nitrate nonahydrate, copper sulphate pentahydrate, titanium tetrachloride, thiourea, potassium peroxodisulphate (PDS), hydrogen peroxide (H_2O_2) and sodium hydroxide were received from Merck, India.

Preparation of sulphur-doped titania catalyst

Initially, $TiCl_4$ (0.05 M) was added drop-wise into 400 mL double distilled water while it was surrounded by an ice bath. After stirring for several minutes, 0.12 M thiourea (source for sulphur) solution was added drop-wise into the above solution and proper stirring was maintained for 30 min. The obtained sol was kept overnight for aging. The precipitate formed was filtered, washed (to remove the chloride content), dried at 343 K, and finally calcined for 3 h at 673 K to obtain the sulphur-doped TiO_2 photocatalyst. The colour of the prepared S-doped titanium dioxide powder sample was pale yellow.

Photocatalyst characterization

The phase purity of the prepared samples were analyzed by recording powder X-ray diffraction (XRD) patterns on a Xpert-Pro diffractometer with Cu Kα radiation ($\lambda = 1.5405$ Å) in the 2θ range of 10–80° at a scan rate of 0.02° s^{-1}. A Shimadzu 2550 UV-visible spectrophotometer equipped with a diffuse reflectance accessory (ISR 2200) was used to obtain the diffuse reflectance spectra of the catalyst over a range of 300–600 nm.

Photodegradation studies

The photodegradation experiments were carried out in a photocatalytic chamber provided with magnetic stirrer (to maintain uniform suspension) and four cooling fans (11 cm diameter). Tungsten-halogen lamp (250 W, Philips, India) was used for the continuous emission of visible light ($\lambda = 360$–2000 nm). The UV radiation ($\lambda < 395$ nm) was filtered using a 2 Mil (50 μm thick) CU clear sun-control film (Garware, India). A photochemical reactor made of borosilicate glass (125 mL) was used. 70 mL of dye solution (in double distilled water) of appropriate concentration was taken within the photoreactor. Ferric or cupric ion solution with desired concentration and/or photocatalyst (TiO_2 or sulphur-doped TiO_2 (S–TiO_2)) was introduced into the photoreactor and then the solution mixture was stirred continuously for 45 min in dark to ensure adsorption/desorption equilibrium. Finally, oxidants (PMS or PDS or H_2O_2) were introduced into the above suspension just before light irradiation. The dye concentration (determined spectrophotometrically using a Shimadzu 2550 UV-vis spectrophotometer; from the absorbance of the dye at its $\lambda_{max} = 543$ nm; $\varepsilon_{max} = 25,000$ M^{-1} cm^{-1}) in bulk solution at this condition (just before starting light irradiation) is used as the initial concentration (C_0). During the irradiation, 5 mL aliquots were withdrawn at appropriate time intervals and the photocatalyst was removed immediately by centrifugation and filtration through syringe filter (0.2 μm). The concentration obtained at a certain irradiation time (t) is denoted as C_t. Total organic carbon (TOC) was measured using a Shimadzu TOC–V_{CPH} model TOC analyzer. pH of the suspension was adjusted to 5.6 using dilute NaOH solution.

RESULTS AND DISCUSSION

Characterization of S-TiO_2 particles

The X-ray diffraction patterns of S-TiO_2 calcined at 400 °C is shown in Figure 1. The observed XRD peaks correspond to those indexed for (1 0 1), (0 0 4),

Current Research Paper

(2 0 0), (1 0 5), (2 1 3), (1 1 6), (2 2 0), (3 0 1) planes of anatase phase of TiO_2 (JCPDS file No. 21-1272). The average grain size of the anatase crystallites estimated by means of Scherrer equation, $D = 0.9\lambda / \beta\cos\theta$ (D - the grain diameter; λ - wavelength of X-ray used; β - full-width at half-maximum of the peak in radians; θ - the angle of diffraction in degree) was found to be 8 nm. The fact that the doped sample exhibit only peaks related to anatase phase reveals that the prepared sample has only anatase crystallites, which is considered to be best photoactive.
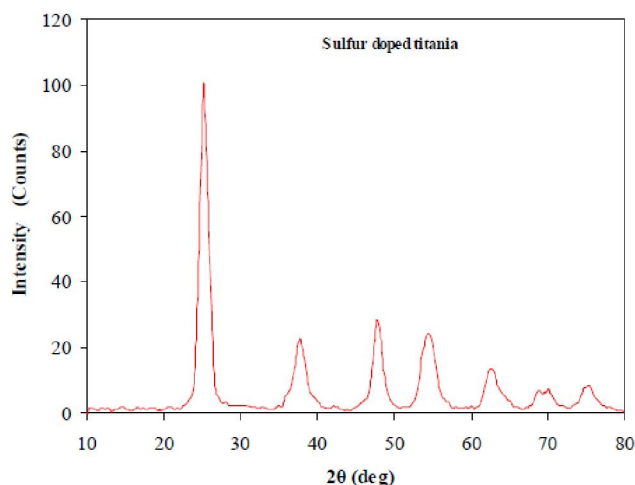

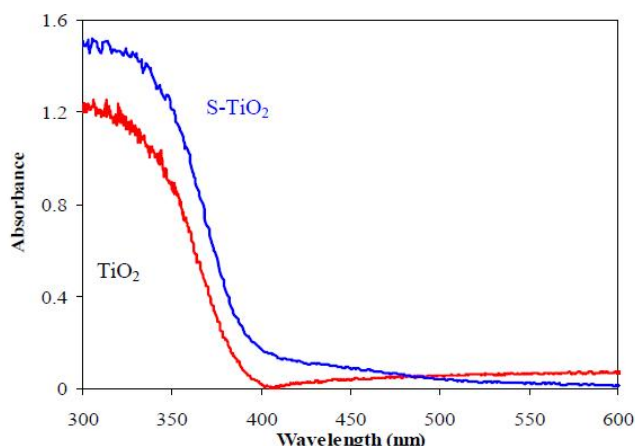**Figure 1 : XRD pattern of S-TiO$_2$ calcined at 400 °C for 3 h.**

Figure 2 : UV-vis absorption spectra of TiO$_2$ (P25) and sulphur-doped TiO$_2$ calcined at 400 °C for 3 h.

Figure 2 shows the diffuse reflectance spectra of S-TiO_2 and undoped TiO_2 particles. The doped catalyst shows a clear shift in the absorption edge towards the visible light range (> 400 nm) which can be attributed to the sulphur doping. This may be due to the substitution of lattice titanium by S^{6+} cation that might have formed an isolated narrow band above the valence band

of TiO_2 which in turn reduces the bandgap[10,11]. When TiO_2 is doped with sulphur, the sulphur 3p states are somewhat delocalized, thus greatly contributing to the formation of the VB with the oxygen 2p and Ti 3d states. Consequently, the mixing of the sulphur 3p states with VB increases the width of the VB itself resulting in a decrease in the bandgap energy[12].

Photodegradation of RR141

A set of experiments were carried out at natural pH (3.2 for TiO_2-Fe^{3+} and 5.5 for TiO_2-Cu^{2+} systems) of the aqueous suspensions. It was observed that, in TiO_2-Fe^{3+}-system, catalyst poisoning occurred due to complete adsorption of the dye molecules on to the catalyst surface since acidic pH is not favorable for TiO_2. But, in TiO_2-Cu^{2+}-system, initial adsorption amount noticed was moderate. When PMS was added into the suspension with TiO_2-Fe^{3+}-dye, initial adsorption was further increased due to the reduction in the pH of the suspension. In TiO_2-Cu^{2+}-system, the extent of adsorption seems to be moderate with better rate of reaction than individual photocatalysis as well as photo-Fenton-like process, as the natural pH of this coupled system falls between 5.4 and 5.8 which is almost same as individual processes. Maximum reaction rate was attained at pH 5.8 for TiO_2 with dye (photocatalysis) whereas in the case of Fe^{3+} and Cu^{2+} based studies (photo-Fenton-like reaction) highest activity was observed at pH 3.2 and 5.5 respectively. In order to improve the rate of reaction as well as to minimize the extent of adsorption, the pH of the TiO_2-Fe^{3+}-oxidant system was altered to ~ 5.6 and it was found that the initial adsorption reduces to a minimum and an enhancement in the rate of reaction compared to individual photocatalysis or photo-Fenton-like reactions was noted. Raising pH to a value above 6 in both the systems had shown a negative impact on pseudo first-order rate constants. Therefore, further studies were carried out by maintaining the pH ~ 5.6 for all the systems (TiO_2-Fe^{3+}-oxidant, TiO_2-Cu^{2+}-oxidant and S-TiO_2-Fe^{3+}/Cu^{2+}-oxidants).

Combination of titania with Fe^{3+} or Cu^{2+} ions alone (without oxidants) in visible light showed detrimental effects on decolourization efficacy. It was observed that the decolourization of RR141 attained after 1 h visible light irradiation using TiO_2-Fe^{3+} or TiO_2-Cu^{2+} systems

was less than 15 percent which was far lower than that obtained using TiO_2 alone (44%). Application of sulphur-doped TiO_2 ($S-TiO_2$) instead of undoped TiO_2 (Degussa P25) along with Fe^{3+} or Cu^{2+} also showed similar results. The retardation of photodegradation rate on addition of Fe^{3+} or Cu^{2+} in TiO_2 based systems may be due to the quenching of photo-generated electrons by the adsorbed metal-ions which act as recombination centers that in turn reduce the generation of active radicals[15]. The strong negative effect on the photodegradation of RR141 can be due to the competition of organic compounds with iron species for adsorption on to TiO_2 surface also. The adverse effect of metal ion deposition on TiO_2 photocatalysis was reported by previous studies[16,17].

An increase in the pseudo first-order rate constant values (compared to individual processes) was observed when TiO_2-Fe^{3+} or TiO_2-Cu^{2+} photocatalysis was performed in the presence of oxidants, namely, oxone (PMS), PDS and H_2O_2, as given in TABLE 1. The enhanced degradation observed in the coupled systems with oxidants ($TiO_2 + Fe^{3+} + Dye + oxidant$ or $TiO_2 + Cu^{2+} + Dye + oxidant$) may be attributed to the enhanced generation of active radicals through decomposition of oxidants by both $TiO_2(e^-)$ and metal ions. In TiO_2 suspension, the dynamic equilibrium between Fe^{3+} and Fe^{2+} (due to the redox reactions with irradiated TiO_2) is reached very fast. In metal-ions mediated photocatalysis, formation of stable dye-metal ion complexes should have favored degradation[18]. Almost complete decolourization was achieved within 30 min in the case of coupled systems ($TiO_2 + Cu^{2+}$ or $Fe^{3+} + Dye + oxidant systems$).

Effect of oxidant concentration

Experiments were carried out with different oxidant concentrations (0.5 to 2.5 mM) at constant dye (5 × 10^{-5} M), TiO_2 (1.428 g L^{-1}) and $S-TiO_2$ (1.428 g L^{-1}) concentrations. Effect of oxidant concentration on pseudo first-order rate constant values during photodegradation of RR141 using combined photocatalytic and photo-Fenton systems are illustrated in Figures. 3 and 4. In coupled systems, increase in the pseudo first-order rate constants was observed till an optimum oxidant concentration beyond which a slight decrement in the pseudo first-order rate constant was noted. Among

the three oxidants chosen, PMS was showing improved activity in the coupled systems. In coupled system that work with $S-TiO_2$, oxidizing potential was considerably increased especially with cupric ions.
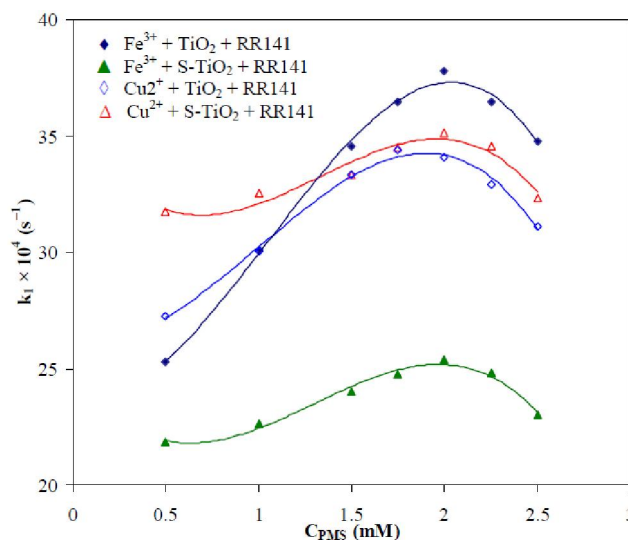

Figure 3 : Effect of PMS concentration on the pseudo first-order rate constants for the photodegradation of RR141 in the coupled system; $[TiO_2] = [S-TiO_2] = 1.428$ g L^{-1}; $[Fe^{3+}] = [Cu^{2+}] = 0.2$ mM; $[RR141] = 5 × 10^{-5}$ M.
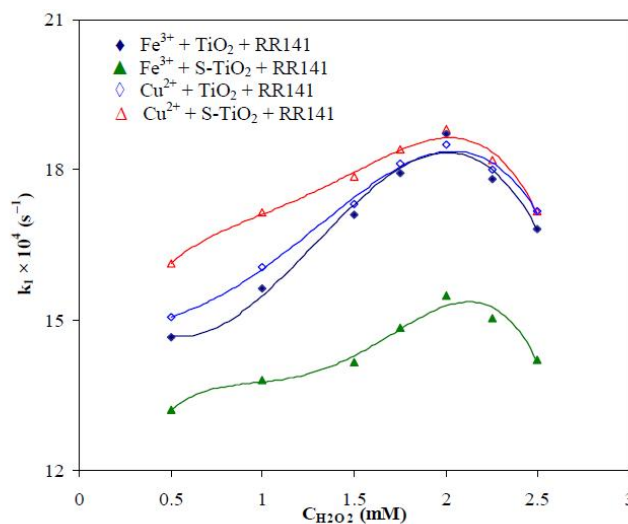

Figure 4 : Effect of H_2O_2 concentration on the pseudo first-order rate constants for the photodegradation of RR141 in the coupled system; $[TiO_2] = [S-TiO_2] = 1.428$ g L^{-1}; $[Fe^{3+}] = [Cu^{2+}] = 0.2$ mM; $[RR141] = 5 × 10^{-5}$ M.

Introducing peroxomonosulphate into the solution leads to the formation of $SO_4^{\bullet-}$ and SO_5^- radicals as well as hydroxyl radicals through radical chain reactions. PDS, a powerful oxidizing agent with a standard potential of $E_0 = 2.01$ V, can be decomposed to SO_4^{2-} ion and $SO_4^{\bullet-}$ by the photo-generated e^- present in TiO_2

Current Research Paper

as well as by metal ions. The $SO_4^{\cdot-}$ radical has the ability to attack organic compounds by abstraction of a hydrogen atom or addition on unsaturated molecules. The initial increase in the degradation efficiency that accompanies with the addition of oxidants can be attributed to the increased formation of $^\cdot OH$ radicals[19] as explained earlier. The reduction in the rate constants noted in the presence of oxone, beyond optimum concentration, may be due to the destruction of sulphate and hydroxyl radicals by the excess HSO_5^-. Higher oxidant concentration reduces the apparent rate constant due

to the scavenging effect of hydroxyl and sulphate radicals themselves as well as by the Fe^{2+} ions in the solution[14]. The overdose of H_2O_2 retards the photocatalytic degradation rates since at higher H_2O_2 concentrations, the hydrogen peroxide adsorbed on the photocatalyst surface could effectively scavenge the $^\cdot OH$ radicals and finally forms a much weaker oxidant $HO_2^\cdot$ thereby inhibiting the major pathway for the generation of $^\cdot OH$ radicals[20,21].

Increment in decolourization achieved with PDS in coupled system is well appreciable. A 2.4-fold raise in the rate constants when compared to individual processes was recorded (TABLE 1). Sulphate radicals have a longer half life than hydroxyl radicals mainly due to their preference for electron transfer reactions while hydroxyl radicals can participate in a variety of reactions with equal preference. The high oxidation efficiencies of the $SO_4^{\cdot-}$ radicals in combination with the slow rate of consumption of precursor oxidants (due to their stability) make sulphate radical based processes very effective for the degradation of recalcitrant organic compounds[22].

TABLE 1 : The pseudo first-order rate constants and mineralization amounts obtained in photocatalysis, photo-fenton like reactions and combined systems (TiO_2 or S-TiO_2–Fe^{3+}–oxidant & TiO_2 or S-TiO_2–Cu^{2+}–oxidant) under optimized conditions.

Catalyst	Photodegradation rate constant $k_1 \times 10^4$ (s^{-1})	Mineralization Efficiency after 4 h (%)
TiO_2	1.87	42
S–TiO_2	4.77	57
TiO_2 + PMS	17.1	68
S–TiO_2 + PMS	25.1	69
Fe^{3+} + PMS	27.18	80
Cu^{2+} + PMS	16.12	76
TiO_2 + Fe^{3+} + PMS	37.78	88
TiO_2 + Cu^{2+} + PMS	34.37	90
S–TiO_2 + Fe^{3+} + PMS	25.38	87
S–TiO_2 + Cu^{2+} + PMS	35.13	91
TiO_2 + PDS	3.10	63
S–TiO_2 + PDS	5.50	59
Fe^{3+} + PDS	8.680	74
Cu^{2+} + PDS	5.970	64
TiO_2 + Fe^{3+} + PDS	20.57	88
TiO_2 + Cu^{2+} + PDS	21.67	87
S–TiO_2 + Fe^{3+} + PDS	19.43	80
S–TiO_2 + Cu^{2+} + PDS	22.78	85
TiO_2 + H_2O_2	5.10	63
S–TiO_2 + H_2O_2	8.07	64
Fe^{3+} + H_2O_2	12.33	76
Cu^{2+} + H_2O_2	5.770	70
TiO_2 + Fe^{3+} + H_2O_2	18.72	84
TiO_2 + Cu^{2+} + H_2O_2	18.50	86
S–TiO_2 + Fe^{3+} + H_2O_2	15.50	83
S–TiO_2 + Cu^{2+} + H_2O_2	18.82	87

Foot note: $[TiO_2]$ = $[S$-$TiO_2]$ = 1.428 g L^{-1}; $[Fe^{3+}]$ = $[Cu^{2+}]$ = 0.2 mM; [RR141] = 5×10^{-5} M; [Oxidants] = 2 mM.

CONCLUSIONS

Integration of titanium dioxide based photocatalysis with Fe^{3+} or Cu^{2+}-oxidant systems seems to be effective and promising approach for the removal of azo-dyes. The degradation is favored at a pH of 5.6 by TiO_2 or S-TiO_2-Fe^{3+}-oxidant or TiO_2 or S-TiO_2-Cu^{2+}-oxidant systems. In the case of coupled systems, complete decolourization can be achieved within 30 min while individual systems took more time for complete colour removal. Combination of titania photocatalyst with photo-Fenton-like process produces a synergic effect that leads to increase in photodegradation rate constant to a value which is larger than those obtained for these AOPs when performed separately, may be due to the generation of radicals through decomposition of oxidants by both excited titania and metal-ions.

ACKNOWLEDGEMENTS

Current Research Paper

REFERENCES

[1] J.Madhavan, F.Grieser, M.Ashokkumar; Degradation of orange-G by advanced oxidation processes, Ultrason.Sonochem, **17**, 338–343 **(2010)**.

[2] S.Mozia, A.W.Morawski, M.Toyoda, T.Tsumura; Integration of photocatalysis and membrane distillation for removal of mono and poly-azo dyes from water, Desalination, **250**, 666–672 **(2010)**.

[3] J.Ramirez, L.A.Godinez, M.Mendez, Y.Meas, F.J.Rodriguez; Heterogeneous photo-electro-Fenton process using different iron supporting materials, J.Appl.Electrochem., **40**, 1729–1736 **(2010)**.

[4] P.J.D.Ranjit, K.Palanivelu, C.S.Lee; Degradation of 2,4-dichlorophenol in aqueous solution by sono-Fenton method, Korean J.Chem.Eng., **25**, 112–117 **(2008)**.

[5] A.Lahkimi, M.A.Oturan, N.Oturan, M.Chaouch; Removal of textile dyes from water by the electro-Fenton process, Environ.Chem.Lett., **5**, 35–39 **(2007)**.

[6] K.P.Mishra, P.R.Gogate; Intensification of sonophotocatalytic degradation of p-nitrophenol at pilot scale capacity, Ultrason.Sonochem., **18**, 739–744 **(2011)**.

[7] H.Mestankova, G.Mailhot, J.Jirkovsky, J.Krysa, M.Bolte; Effect of iron speciation on the photodegradation of monuron in combined photocatalytic systems with immobilized or suspended TiO_2, Environ.Chem.Lett., **7**, 127–132 **(2009)**.

[8] R.Asahi, T.Morikawa, T.Ohwaki, K.Aoki, Y.Taga; Visible-light photocatalysis in nitrogen-doped titanium oxides, Science, **293**, 269–271 **(2001)**.

[9] D.B.Hamal, K.J.Klabunde; Synthesis, characterization, and visible light activity of new nanoparticle photocatalysts based on silver, carbon, and sulphur-doped TiO_2, J.Colloid Inter.Sci., **311**, 514–522 **(2007)**.

[10] S.Liu, X.Chen; Visible light response TiO_2 photocatalyst realized by cationic S-doping and its application for phenol degradation, J. azard.Mater., **152**, 48–55 **(2007)**.

[11] T.Umebayashi, T.Yamaki, H.Itoh, K.Asai; Bandgap narrowing of titanium dioxide by sulphur doping, Appl.Phys.Lett., **81**, 454–456 **(2002)**.

[12] M.S.Wong, S.W.Hsu, K.K.Rao, C.P.Kumar; Influence of crystallinity and carbon content on visible light photocatalysis of carbon doped titania thin films, J.Mol.Catal.A: Chem., **279**, 20–26 **(2008)**.

[13] G.P.Anipsitakis, D.Dionysiou; Degradation of organic contaminants in water with sulphate radicals generated by the conjunction of peroxymonosulphate with cobalt, Environ.Sci.Technol., **37**, 4790–4797 **(2003)**.

[14] L.G.Devi, S.G.Kumar, K.M.Reddy; Photo Fenton like process $Fe^{3+}/(NH_4)2S_2O_8$ / UV for the degradation of di azo dye congo red using low iron concentration, Cent.Eur.J.Chem., **7**, 468–477 **(2009)**.

[15] M.R.Dhananjeyan, V.Kandavelu, R.Renganathan; An investigation of the effects of Cu^{2+} and heat treatment on TiO_2 photooxidation of certain pyrimidines, J.Mol.Catal.A: Chem., **158**, 577–582 **(2000)**.

[16] P.Bouras, E.Stathatos, P.Lianos; Pure versus metal-ion-doped nanocrystalline titania for photocatalysis, Appl.Catal.B: Environ., **73**, 51–59 **(2007)**.

[17] Q.Yang, H.Choi, Y.Chen, D.D.Dionysiou; Heterogeneous activation of peroxymonosulphate by supported cobalt catalyst for the degradation of 2,4-dichlorophenol in water: The effect of support, cobalt precursor, and UV radiation, Appl.Catal.B: Environ., **77**, 300–307 **(2008)**.

[18] J.Madhavan, F.Grieser, M.Ashokkumar; Degradation of formetanate hydrochloride by combined advanced oxidation processes, Sep.Purif.Technol., **73**, 409–414 **(2010)**.

[19] G.Li, X.S.Zhao, M.B.Ray; Advanced oxidation of orange II using TiO_2 supported on porous adsorbents: The role of pH, H_2O_2 and O_3, Sep.Purif.Technol., **55**, 91–97 **(2007)**.

[20] K.Soutsas, V.Karayannis, I.Poulios, A.Riga, K.Ntampegliotis, X.Spiliotis, G.Papapolymerou; Decolourization and degradation of reactive azo dyes via heterogeneous photocatalytic processes, Desalination, **250**, 345–350 **(2010)**.

[21] C.S.Turchi, D.F.Ollis; Photocatalytic degradation of organic water contaminants: Mechanisms involving hydroxyl radical attack, J.Catal., **122**, 178–192 **(1990)**.

[22] A.Rastogi, S.R.Al-Abed, D.D.Dionysiou; Sulphate radical-based ferrous–peroxymonosulphate oxidative system for PCBs degradation in aqueous and sediment systems, Appl.Catal., **B85**, 171–179 **(2009)**.